Inorganic Chemistry

pubs.acs.org/IC

Communication

Aluminum-Substituted Keggin Germanotungstate $[HAl(H_2O)GeW_{11}O_{39}]^{4-}$: Synthesis, Characterization, and Antibacterial Activity

Elias Tanuhadi, Nadiia I. Gumerova, Alexander Prado-Roller, Markus Galanski, Hana Čipčić-Paljetak, Donatella Verbanac, and Annette Rompel*

Cite This: *Inorg. Chem.* 2021, 60, 28−31

Read Online

ACCESS | Metrics & More | Article Recommendations | Supporting Information

ABSTRACT: We report on the new monosubstituted aluminum Keggin-type germanotungstate $(C_4H_{12}N)_4[HAlGeW_{11}O_{39}(H_2O)]\cdot 11H_2O$ ($[\mathbf{Al(H_2O)GeW_{11}}]^{4-}$), which has been synthesized at room temperature via rearrangement of the dilacunary $[\gamma\text{-}GeW_{10}O_{36}]^{8-}$ polyoxometalate precursor. $[\mathbf{Al(H_2O)GeW_{11}}]^{4-}$ has been characterized thoroughly both in the solid state by single-crystal and powder X-ray diffraction, IR spectroscopy, thermogravimetric analysis, and elemental analysis as well as in solution by cyclic voltammetry (CV) ^{183}W, ^{27}Al NMR and UV−vis spectroscopy. A study on the antibacterial properties of $[\mathbf{Al(H_2O)GeW_{11}}]^{4-}$ and the known aluminum(III)-centered Keggin polyoxotungstates (Al-POTs) α-$Na_5[AlW_{12}O_{40}]$ ($\boldsymbol{\alpha}$-$[\mathbf{AlW_{12}O_{40}}]^{5-}$) and $Na_6[Al(AlOH_2)W_{11}O_{39}]$ ($[\mathbf{Al(AlOH_2)W_{11}O_{39}}]^{6-}$) revealed enhanced activity for all three Al-POTs against the Gram-negative bacterium *Moraxella catarrhalis* (minimum inhibitory concentration (MIC) up to 4 μg mL^{-1}) and the Gram-positive *Enterococcus faecalis* (MIC up to 128 μg mL^{-1}) compared to the inactive $Al(NO_3)_3$ salt (MIC > 256 μg mL^{-1}). CV indicates the redox activity of the Al-POTs as a dominating factor for the observed antibacterial activity with increased tendency to reduction, resulting in increased antibacterial activity of the POT.

Polyoxometalates (POMs)[1] represent a broad class of anionic inorganic clusters with versatile structural topologies resulting in a variety of chemical and physical properties that can be modulated by molecular design. These features make them attractive materials in a wide range of fields like catalysis,[2] electrochemistry,[3] magnetochemistry,[4] and biological chemistry[5] including protein crystallography.[6] Among the variety of POMs reported to date, Keggin-type POMs represent the largest family. The incorporation of metal ions into the vacant site(s) of lacunary POMs derived from their plenary counterparts upon controlled hydrolysis of the framework is one of the most powerful synthetic approaches used to encapsulate well-defined metal sites with heteroatoms ranging from 3d transition metals over lanthanides to main-group III elements.[1] Regarding the number of main-group-III-containing POMs reported to date, only a few examples deal with the preparation and full structural characterization of aluminum(III)-substituted POMs (Al-POMs; Table S1) due to hydrolysis of the aluminum species in an aqueous environment.[7] Most of the reported Al-POMs have been studied toward their properties as Lewis catalysts,[8] where the incorporation of a high-sensitivity NMR-active ^{27}Al nucleus into the metal−oxo framework allows for detailed speciation and stability studies of the catalytic species. In contrast to catalytic studies, the biological applications of Al-POMs have not been investigated yet.[1] Among the investigated biological applications, the antibacterial properties of POMs have been a subject of growing interest[5] considering the continuing emergence of antibacterial resistance worldwide due to excessive or improper use of antibiotics. Because of their high negative charge, strong acidity, and geometry, POMs offer alternative modes of antimicrobial action by exhibiting synergy with some conventional antibiotics or direct antibacterial activity against both Gram-negative and Gram-positive bacteria.[5,9] Only a few all-inorganic POMs have been shown to exhibit antibacterial activity (Table S2) on their own accord[5] despite their higher water solubility, which would make them more attractive for application in biological systems compared to their hybridized counterparts. Herein, we report the synthesis and thorough characterization of a new monosubstituted Keggin-type germanotungstate, $(C_4H_{12}N)_4[HAl^{III}GeW_{11}O_{39}(H_2O)]\cdot 11H_2O$ ($[\mathbf{Al(H_2O)GeW_{11}}]^{4-}$), which was subjected to an antibacterial study.

The synthesis of $[\mathbf{Al(H_2O)GeW_{11}}]^{4-}$ starts with the preparation of the literature-known dilacunary germanotungstate building block $K_8[\gamma\text{-}GeW_{10}O_{36}]\cdot 12H_2O$ ($\mathbf{GeW_{10}}$).[10] The addition of 2 equiv of $Al(NO_3)_3\cdot 9H_2O$ to a stirred reaction mixture of 1 equiv of $\mathbf{GeW_{10}}$ (pH 7.2) resulted in a significant decrease of the pH value from 7.2 to 3.0. Readjustment of the pH value to pH 3.8 via the dropwise addition of a K_2CO_3 solution (2 M) led to the in situ rearrangement of $\mathbf{GeW_{10}}$ to the monolacunary $[\beta_2\text{-}GeW_{11}O_{39}]^{8-}$ ($\mathbf{GeW_{11}}$) POM species,

Received: November 7, 2020
Published: December 17, 2020

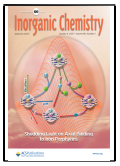

https://dx.doi.org/10.1021/acs.inorgchem.0c03311
Inorg. Chem. 2021, 60, 28−31

Scheme 1. Schematic Representation Showing the Syntheses of $[Al(H_2O)GeW_{11}]^{4-}$[a]

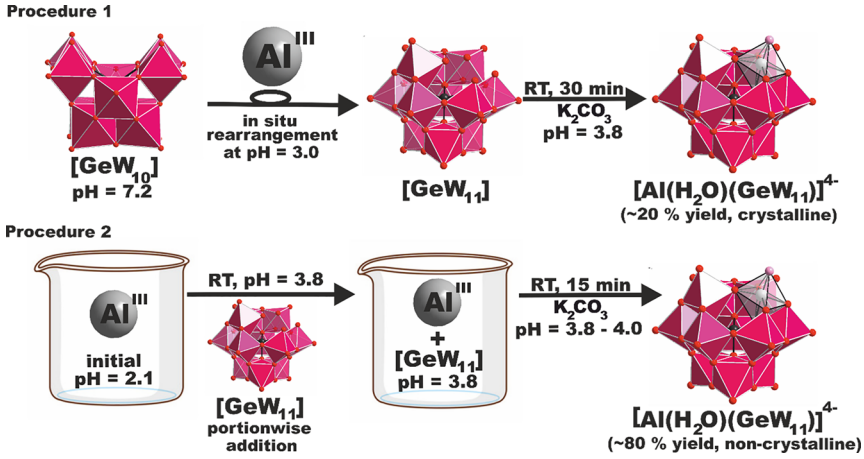

[a] $[Al(H_2O)GeW_{11}]^{4-}$ can be obtained as single crystals suitable for single-crystal X-ray crystallography via rearrangement of the dilacunary $[GeW_{10}]$ precursor (procedure 1) in a yield of 20% based on tungsten. The portionwise addition of the monolacunary $[GeW_{11}]$ to a solution of $Al(NO_3)_3$ leads to the isolation of $[Al(H_2O)GeW_{11}]^{4-}$ in higher yields of 80% based on tungsten (procedure 2). The pH was kept at 3.8−4.0 in both procedures via the constant addition of K_2CO_3 solution (2 M). Black and red spheres represent the germanium(IV) and oxygen ions, respectively. Gray transparent octahedra for aluminum(III) and magenta polyhedra for $\{WO_6\}$.

which incorporates an aluminum(III) metal center and crystallizes as the pure tetramethylammonium (TMA) salt (CCDC 1936850) in a 20% yield based on tungsten (procedure 1). The in situ formation of the GeW_{11} unit can be explained by the pH decrease upon the addition of $Al(NO_3)_3$ to the reaction mixture (procedure 1, Scheme 1).[10] Using the GeW_{11} unit as a precursor, the yield of the desired $[Al(H_2O)GeW_{11}]^{4-}$ was optimized (procedure 2). To avoid the undesired isomerization of the GeW_{11} building block, $Al(NO_3)_3$ was initially dissolved in water, giving an acidic solution of pH 2.1. The portionwise addition of GeW_{11} increases the pH to 3.8, which was kept in the range between 3.8 and 4.0 via the subsequent addition of a K_2CO_3 solution (2 M) over a time period of 15 min to ensure integrity of the GeW_{11} unit and further formation of the desired $[Al(H_2O)GeW_{11}]^{4-}$ anion. The analytically pure $[Al(H_2O)GeW_{11}]^{4-}$ was precipitated as the TMA salt, thereby giving increased yields of 80% based on tungsten compared to synthetic procedure 1 starting from GeW_{10} (Figure S2).

Single-crystal X-ray diffraction (SXRD) measurements were performed on single crystals obtained from procedure 1, revealing that $[Al(H_2O)GeW_{11}]^{4-}$ crystallizes in the monoclinic space group $P21/c$ (Tables S3−S5). The crystal structure of $[Al(H_2O)GeW_{11}]^{4-}$ represents a monosubstituted β_2-Keggin-type polyanion with idealized C_1 symmetry. Occupation of the vacant site with aluminum(III) results in the monosubstituted Keggin-type architecture. The aluminum(III) metal center exhibits a distorted octahedral coordination environment with one terminal H_2O ligand and Al−O bond lengths ranging from 1.823 to 2.037 Å and shows a disorder with tungsten in a 90:10 aluminum/tungsten ratio. Powder XRD measurements were performed on $[Al(H_2O)GeW_{11}]^{4-}$ and compared to the corresponding simulated spectrum, thereby showing the homogeneity of the bulk sample (Figure S4). Besides XRD, $[Al(H_2O)GeW_{11}]^{4-}$ was characterized in the solid state by attenuated-total-reflectance IR spectroscopy (Figure S1), showing the terminal W═O and bridging W−O−W vibrations typical for the Keggin-type polyoxotungstate framework. The bands at 1630 and 2960 cm^{-1} are attributed to the vibration and deformation bands of TMA methyl groups. The number of water molecules in $(C_4H_{12}N)_4[HAl^{III}GeW_{11}O_{39}(H_2O)]\cdot 11H_2O$ was determined using thermogravimetric analysis (TGA). The two weight-loss regions (Figure S3) are attributed to losses of 11 water and 4 TMA molecules, respectively. The UV−vis spectrum of $[Al(H_2O)GeW_{11}]^{4-}$ is characterized by an absorption maximum at 275 nm attributed to the $p_\pi(O_b) \rightarrow d_\pi^*(W)$ ligand-to-metal charge-transfer typical for the Keggin-type framework (Figure S5).[11] The ^{183}W NMR spectrum of a freshly prepared aqueous solution (pH 6.8) of $[Al(H_2O)GeW_{11}]^{4-}$ (18.4 mM) reveals the domination of $[Al(H_2O)GeW_{11}]^{4-}$ in solution, which possesses C_1 symmetry and gives rise to 11 ^{183}W NMR signals (all tungsten atoms are chemically unique; Figure 1).[12] The additional signal at −84.3 ppm (6.5% based on integration values) can be assigned to α-$[GeW_{12}O_{40}]^{4-}$, which is in accordance with the shift at −81.9 ppm previously described in the literature.[13] ^{27}Al NMR

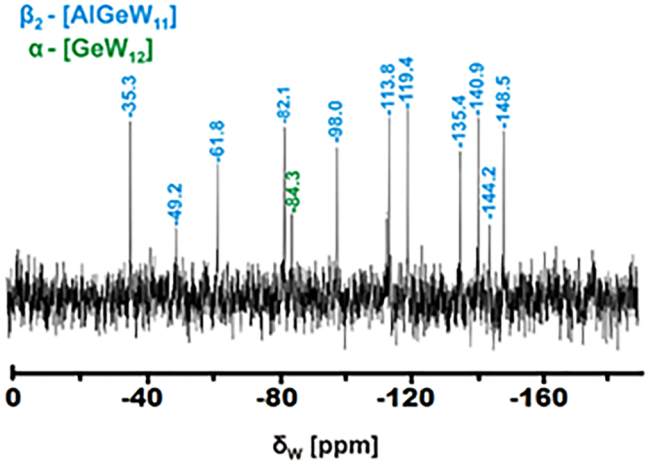

Figure 1. ^{183}W NMR spectrum of $[Al(H_2O)GeW_{11}]^{4-}$ in D_2O at pH 6.8. Signal assignment was according to refs 12 and 13. $[Al(H_2O)GeW_{11}]^{4-}$ was dissolved in water to obtain a 60 mg mL^{-1} solution (18.4 mM). The total recording time was 60 h, and the chemical shifts were measured relative to an external 1 M Na_2WO_4 standard.

https://dx.doi.org/10.1021/acs.inorgchem.0c03311
Inorg. Chem. 2021, 60, 28−31

measurements were performed on $[Al(H_2O)GeW_{11}]^{4-}$ dissolved in D_2O (pH 6.8), revealing one broad peak at 10.2 ppm, which can be attributed to the octahedrally coordinated aluminum(III) present in $[Al(H_2O)GeW_{11}]^{4-}$ (Figure S6).

Considering the solution stability of $[Al(H_2O)GeW_{11}]^{4-}$ under physiological conditions (pH 6.8), antibacterial studies against *Moraxella catarrhalis*, a Gram-negative human mucosal pathogen that causes middle ear infections in children,[14] and *Enterococcus faecalis*, a Gram-positive bacterium responsible for life-threatening sepsis and urinary tract and meningitis infections,[15] were performed. For comparability of the antibacterial activity of $[Al(H_2O)GeW_{11}]^{4-}$, the literature-known aluminum-substituted polyoxotungstates (Al-POTs) α-$[AlW_{12}O_{40}]^{5-}$ and α-$[Al(AlOH_2)W_{11}O_{39}]^{6-}$ synthesized and characterized by Weinstock et al.[12] were prepared, and their purity and stability at physiological pH were proven by ^{27}Al NMR spectroscopy (Figures S7 and S8). ^{27}Al NMR measurements were performed on solutions of the Al-POTs incubated in the Müller–Hinton–Bouillon (MHB) medium[16] (pH 7.4) at 37 °C overnight to recreate the conditions used for the antibacterial tests. The ^{27}Al NMR spectra of $[Al(AlOH_2)W_{11}O_{39}]^{6-}$, α-$[AlW_{12}O_{40}]^{5-}$, and $[Al(H_2O)GeW_{11}]^{4-}$ in a 50% D_2O/MHB medium solution remain unchanged (Figures S9–S11). All three Al-POTs reveal enhanced antibacterial activity in the order α-$[Al(AlOH_2)W_{11}O_{39}]^{6-}$ < $[Al(H_2O)GeW_{11}]^{4-}$ < α-$[AlW_{12}O_{40}]^{5-}$ compared to the inactive $Al(NO_3)_3$ (Table S7). In contrast to the expected trend that would suggest increased antibacterial activity with an increasing negative charge of the corresponding polyanion,[17] α-$[AlW_{12}O_{40}]^{5-}$ exhibits the overall highest activity with minimum inhibitory values of MIC = 4 μg mL^{-1} against *M. catarrhalis* (Table S7) and MIC = 128 μg mL^{-1} against *E. faecalis*. For a better understanding of the observed trend, cyclic voltammetry (CV) was performed on 2 mM solutions of $[Al(H_2O)GeW_{11}]^{4-}$, α-$[AlW_{12}O_{40}]^{5-}$, and $[Al(AlOH_2)W_{11}O_{39}]^{6-}$ in a MHB medium, revealing three reversible redox waves attributed to tungsten(VI)/tungsten(V) transitions (Table S6 and Figures S12–S14) for all representatives, with a clear shift of the peak cathodic currents to more positive potentials in the order α-$[Al(AlOH_2)W_{11}O_{39}]^{6-}$ < $[Al(H_2O)GeW_{11}]^{4-}$ < α-$[AlW_{12}O_{40}]^{5-}$, which is in accordance with the observed activity trend of the Al-POTs (Figure 2). On the basis of the CV measurements, the activity trend can be explained by the different redox activity of the POTs with increased tendency to reduction, resulting in an increased antibacterial activity of the POT. Considering the charge densities q/M (charge q divided by the number of tungsten atoms M) of the polyanions (0.36 for $[Al(H_2O)GeW_{11}]^{4-}$, 0.42 for α-$[AlW_{12}O_{40}]^{5-}$, and 0.54 for $[Al(AlOH_2)W_{11}O_{39}]^{6-}$), recent findings show that POMs, as superchaotropes, with intermediate charge density (q/M = 0.4) interact considerably strongly with various surfaces of different or mixed polarities[18] such as the bacterial cytoskeleton of the Gram-positive *E. faecalis*, rendering the intact α-$[AlW_{12}O_{40}]^{5-}$ (q/M = 0.42) and $[Al(H_2O)GeW_{11}]^{4-}$ (q/M = 0.36) to exhibit the highest activity (MIC = 128 μg/mL) out of the series.

In conclusion, the new monosubstituted Keggin-based aluminogermanotungstate $[Al(H_2O)GeW_{11}]^{4-}$ was synthesized and thoroughly characterized in the solid state and solution. A study on the antibacterial activity of $[Al(H_2O)GeW_{11}]^{4-}$, α-$[AlW_{12}O_{40}]^{5-}$, and α-$[Al(AlOH_2)W_{11}O_{39}]^{6-}$ revealed the redox activity of the polyanions to be a crucial factor determining the overall antibacterial activity. These findings highlight the importance of lacunary POMs as all-inorganic ligands, which can be used to tune the redox behavior of otherwise antibacterially inactive metal centers such as Al.

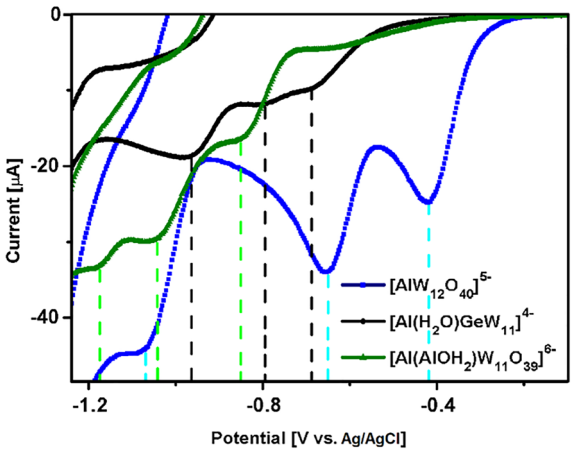

Figure 2. Superimposed cyclic voltammograms of α-$[Al(AlOH_2)W_{11}O_{39}]^{6-}$, $[Al(H_2O)GeW_{11}]^{4-}$, and α-$[AlW_{12}O_{40}]^{5-}$ in a MHB medium at pH 6.8. Working electrode, glassy carbon (d = 3 mm); reference electrode, Ag/AgCl; scan rate, 50 mV s^{-1}; concentration of POMs, 2 mM.

■ ASSOCIATED CONTENT

Supporting Information

The Supporting Information is available free of charge at https://pubs.acs.org/doi/10.1021/acs.inorgchem.0c03311.

Details on the syntheses, TGA, XRD, CV, IR, UV–vis, and NMR spectroscopy, and antibacterial studies (PDF)

Accession Codes

CCDC 1936850 contains the supplementary crystallographic data for this paper. These data can be obtained free of charge via www.ccdc.cam.ac.uk/data_request/cif, or by emailing data_request@ccdc.cam.ac.uk, or by contacting The Cambridge Crystallographic Data Centre, 12 Union Road, Cambridge CB2 1EZ, UK; fax: +44 1223 336033.

■ AUTHOR INFORMATION

Corresponding Author

Annette Rompel − *Universität Wien, Fakultät für Chemie, Institut für Biophysikalische Chemie, 1090 Wien, Austria;* orcid.org/0000-0002-5919-0553; Email: annette.rompel@univie.ac.at

Authors

Elias Tanuhadi − *Universität Wien, Fakultät für Chemie, Institut für Biophysikalische Chemie, 1090 Wien, Austria*

Nadiia I. Gumerova − *Universität Wien, Fakultät für Chemie, Institut für Biophysikalische Chemie, 1090 Wien, Austria*

Alexander Prado-Roller − *Universität Wien, Fakultät für Chemie, Institut für Anorganische Chemie und Zentrum für Röntgenstrukturanalyse, 1090 Wien, Austria*

Markus Galanski − *Universität Wien, Fakultät für Chemie, Institut für Anorganische Chemie und NMR Zentrum, 1090 Wien, Austria*

Hana Cipčić-Paljetak − *Center for Translational and Clinical Research, Croatian Center of Excellence for Reproductive and*

https://dx.doi.org/10.1021/acs.inorgchem.0c03311
Inorg. Chem. 2021, 60, 28–31

Regenerative Medicine, School of Medicine, University of Zagreb, 10000 Zagreb, Croatia

Donatella Verbanac − *Faculty of Pharmacy and Biochemistry, University of Zagreb, 10000 Zagreb, Croatia*

Complete contact information is available at: https://pubs.acs.org/10.1021/acs.inorgchem.0c03311

Notes

The authors declare no competing financial interest.

■ ACKNOWLEDGMENTS

We gratefully acknowledge the Austrian Science Fund FWF (Grants P27534, P33089, M2203, and P33927) as well as the University of Vienna for financial support. E.T. and A.R. acknowledge the University of Vienna for awarding a Uni:docs fellowship to E.T. Bilateral financial funding was provided by the Centre for International Cooperation & Mobility (ICM) of the Austrian Agency for International Cooperation in Education and Research (OeADGmbH) Project HR 06/2020 to A.R. and the Project "Biological profiling of polyoxometalates" to H.C.-P. Last, the authors thank Heiko Geisler, M.Sc., for assistance with CV measurements, Marek Bujdoš for support with ICP-OES measurements, and Ass. Prof. Dr. Peter Unfried for TGA measurements.

■ REFERENCES

(1) (a) Pope, M. T. *Heteropoly and Isopoly Oxometalates*; Springer Verlag: Berlin, 1983; Vol. 2, pp 10−26. (b) Gumerova, N. I.; Rompel, A. Polyoxometalates in solution: speciation under spotlight. *Chem. Soc. Rev.* **2020**, *49*, 7568−7601.

(2) Wang, S. S.; Yang, G. Y. Recent Advances in Polyoxometalate-Catalyzed Reactions. *Chem. Rev.* **2015**, *115* (11), 4893−4962.

(3) Sadakane, M.; Steckhan, E. Electrochemical Properties of Polyoxometalates as Electrocatalysts. *Chem. Rev.* **1998**, *98* (1), 219−238.

(4) Clemente-Juan, J. M.; Coronado, E.; Gaita-Ariño, A. Magnetic polyoxometalates: from molecular magnetism to molecular spintronics and quantum computing. *Chem. Soc. Rev.* **2012**, *41*, 7464−7478.

(5) (a) Bijelic, A.; Aureliano, M.; Rompel, A. The antibacterial activity of polyoxometalates: structures, antibiotic effects and future perspectives. *Chem. Commun.* **2018**, *54*, 1153−1169. (b) Bijelic, A.; Aureliano, M.; Rompel, A. Polyoxometalates as Potential Next-Generation Metallodrugs in the Combat Against Cancer. *Angew. Chem., Int. Ed.* **2019**, *58*, 2980−2999. (c) Bijelic, A.; Aureliano, M.; Rompel, A. Im Kampf gegen Krebs: Polyoxometallate als nächste Generation metallhaltiger Medikamente. *Angew. Chem.* **2019**, *131*, 3008−3029.

(6) (a) Bijelic, A.; Rompel, A. The use of polyoxometalates in protein crystallography − An attempt to widen a well-known bottleneck. *Coord. Chem. Rev.* **2015**, *299*, 22−38. (b) Bijelic, A.; Rompel, A. Ten Good Reasons for the Use of the Tellurium-Centered Anderson−Evans Polyoxotungstate in Protein Crystallography. *Acc. Chem. Res.* **2017**, *50*, 1441−1448. (c) Bijelic, A.; Rompel, A. Polyoxometalates − More than a phasing tool in protein crystallography. *ChemTexts* **2018**, *4*, 10.

(7) Casey, W. H. Large Aqueous Aluminum Hydroxide Molecules. *Chem. Rev.* **2006**, *106*, 1−16.

(8) (a) Carraro, M.; Bassil, B. S.; Soraru, A.; Berardi, S.; Suchopar, A.; Kortz, U.; Bonchio, M. A Lewis acid catalytic core sandwiched by inorganic polyoxoanion caps: selective H_2O_2-based oxidations with $[Al^{III}_4(H_2O)_{10}(\beta\text{-}XW_9O_{33}H)_2]^{6-}$ (X = As^{III}, Sb^{III}). *Chem. Commun.* **2013**, *49*, 7914−7916. (b) Kikukawa, Y.; Yamaguchi, S.; Nakagawa, Y.; Uehara, K.; Uchida, S.; Yamaguchi, K.; Mizuno, N. Synthesis of a Dialuminum-Substituted Silicotungstate and the Diastereoselective Cyclization of Citronellal Derivatives. *J. Am. Chem. Soc.* **2008**, *130*, 15872−15878.

(9) Dizaj, S. M.; Lotfipour, F.; Barzegar-Jalali, M.; Zarrintan, M. H.; Adibkia, K. Antimicrobial activity of the metals and metal oxide nanoparticles. *Mater. Sci. Eng. C* **2014**, *44*, 278−284.

(10) Nsouli, N. H.; Bassil, B. S.; Dickman, M. H.; Kortz, U.; Keita, B.; Nadjo, L. Synthesis and Structure of Dilacunary Decatungstogermanate, $[\gamma\text{-}GeW_{10}O_{36}]^{8-}$. *Inorg. Chem.* **2006**, *45*, 3858−3860.

(11) Bi, L.; Li, B.; Wu, L.; Bao, Y. Synthesis, characterization and crystal structure of a novel 2D network structure based on hexacopper(II) substituted tungstoantimonate. *Inorg. Chim. Acta* **2009**, *362*, 3309−3313.

(12) Cowan, J. J.; Bailey, A. J.; Heintz, R. A.; Do, B. T.; Hardcastle, K. I.; Hill, C. L.; Weinstock, I. A. Formation, Isomerization, and Derivatization of Keggin Tungstoaluminates. *Inorg. Chem.* **2001**, *40*, 6666−6675.

(13) Bagno, A.; Bonchio, M.; Autschbach, J. Computational Modeling of Polyoxotungstates by Relativistic DFT Calculations of ^{183}W NMR Chemical Shifts. *Chem. - Eur. J.* **2006**, *12*, 8460−8471.

(14) (a) Karalus, R.; Campagnari, A. *Moraxella catarrhalis*: a review of an important human mucosal pathogen. *Microbes Infect.* **2000**, *2*, 547−559.

(15) Ryan, K. J.; Ray, C. J. *Sherris medical microbiology*; McGraw-Hill: London, U.K., 2004.

(16) Mueller, J. H.; Hinton, J. A Protein-Free Medium for Primary Isolation of the *Gonococcus* and *Meningococcus*. *Exp. Biol. Med.* **1941**, *48* (1), 330−333.

(17) Gumerova, N. I.; Al-Sayed, E.; Krivosudský, L.; Čipčić-Paljetak, H.; Verbanac, D.; Rompel, A. Antibacterial activity of polyoxometalates against *Moraxella catarrhalis*. *Front. Chem.* **2018**, *6*, 336.

(18) (a) Assaf, K. I.; Ural, M. S.; Pan, F.; Georgiev, T.; Simova, S.; Rissanen, K.; Gabel, D.; Nau, W. M. Water Structure Recovery in Chaotropic Anion Recognition: High-Affinity Binding of Dodecaborate Clusters to γ-Cyclodextrin. *Angew. Chem., Int. Ed.* **2015**, *54*, 6852−6856. (b) Assaf, K. I.; Nau, W. M. The chaotropic effect as an assembly motif in chemistry. *Angew. Chem., Int. Ed.* **2018**, *57*, 13968−13981. (c) Buchecker, T.; Schmid, P.; Renaudineau, S.; Diat, O.; Proust, A.; Pfitzner, A.; Bauduin, P. Polyoxometalates in the Hofmeister series. *Chem. Commun.* **2018**, *54*, 1833−1836. (d) Solé-Daura, A.; Poblet, J. M.; Carbó, J. J. Structure−Activity Relationships for the Affinity of Chaotropic Polyoxometalate Anions towards Proteins. *Chem. - Eur. J.* **2020**, *26*, 5799−5809. (e) Naskar, B.; Diat, O.; Nardello-Rataj, V.; Bauduin, P. Nanometer-Size Polyoxometalate Anions Adsorb Strongly on Neutral Soft Surfaces. *J. Phys. Chem. C* **2015**, *119*, 20985−20992. (f) Buchecker, T.; Schmid, P.; Grillo, I.; Prévost, S.; Drechsler, M.; Diat, O.; Pfitzner, A.; Bauduin, P. Self-Assembly of Short Chain Poly-N-isopropylacrylamid Induced by Superchaotropic Keggin Polyoxometalates: From Globules to Sheets. *J. Am. Chem. Soc.* **2019**, *141*, 6890−6899.